The Role of Auger Recombination in InAs 1.3-μm Quantum-Dot Lasers Investigated Using High Hydrostatic Pressure

I. P. Marko, A. D. Andreev, A. R. Adams, R. Krebs, J. P. Reithmaier, and A. Forchel

***Abstract*—InAs quantum-dot (QD) lasers were investigated in the temperature range 20–300 K and under hydrostatic pressure in the range of 0–12 kbar at room temperature. The results indicate that Auger recombination is very important in 1.3-μm QD lasers at room temperature and it is, therefore, the possible cause of the relatively low characteristic temperature observed, of $T_0 = 41$ K. In the 980-nm QD lasers where $T_0 = 110$–130 K, radiative recombination dominates. The laser emission photon energy $E_{\rm las}$ increases linearly with pressure p at 10.1 and 8.3 meV/kbar for 980 nm and 1.3-μm QD lasers, respectively. For the 980-nm QD lasers the threshold current increases with pressure at a rate proportional to the square of the photon energy $E_{\rm las}^2$. However, the threshold current of the 1.3-μm QD laser decreases by 26% over a 12-kbar pressure range. This demonstrates the presence of a nonradiative recombination contribution to the threshold current, which decreases with increasing pressure. The authors show that this nonradiative contribution is Auger recombination. The results are discussed in the framework of a theoretical model based on the electronic structure and radiative recombination calculations carried out using an 8×8 k·p Hamiltonian.**

***Index Terms*—Auger recombination, hydrostatic high pressure, InAs, quantum dot, recombination mechanisms, semiconductor laser, threshold current.**

I. Introduction

QUANTUM-DOT (QD) lasers are receiving a great deal of attention, largely due to the low threshold current $I_{\rm th}$ and high temperature stability of quantum dots lasers predicted theoretically almost 20 years ago [1], [2]. This is particularly important for telecommunication systems in which devices are designed to operate at 1.3 μm, where optical fibers have zero dispersion. The main driving reason for reduction of the effective dimensionality of the active regions of semiconductor lasers has been the control of the electron density of states that quantum confinement provides, allowing injected electrons and holes to be ever more restricted to those energies where they can take part in the stimulated emission process. This results, for example, in the prediction that if the electrons can be confined to a single discrete atomic like level in QD lasers, they will not suffer thermal broadening and the threshold current will be temperature insensitive [1], [2]. However, despite the growth of very good self-assembled layers of quantum dots, the longer wavelength lasers required for optical communication remain stubbornly temperature sensitive [3]–[5]. Although nearly temperature insensitive performance was indeed observed in 1.3-μm QD lasers in the temperature range of 100–200 K [3], [5], at room temperature the lasers studied in [3] exhibit an even worse temperature performance than available quantum well devices. At higher temperatures, the characteristic temperature T_0 of the 1.3-μm QD lasers decreases to 30–160 K [3]–[5]. Therefore, it is very important to understand the physical mechanisms responsible for QD laser operation at higher (>250 K) temperatures. A re-emission of carriers into the optical confinement layers (OCL) activated at increasing temperature and their radiative recombination in the OCL was proposed as the reason for the high temperature sensitivity of QD lasers [6], [7]. Recently, it has been shown also that to decrease the temperature sensitivity of $I_{\rm th}$, the shape of the QDs should be engineered to maximize the energy separation between the ground electron and hole states and their respective excited states [8]. In addition, the same group has shown that using p-type doping of the QD active region to avoid gain saturation can increase the characteristic temperature up to $T_0 = 213$ K [9].

In this paper, we show results, from studies of the hydrostatic pressure dependence of the characteristics of 980 nm and 1.3-μm QD lasers, that indicate that strong Auger recombination processes occur in the 1.3-μm lasers where the total threshold current is very temperature dependent. Therefore, the existence of Auger recombination in 1.3-μm QD devices may explain their strong temperature dependence, just as was observed in quantum well 1.3-μm devices [10], [11]. This would be extremely important for their further development since it implies that even if perfectly uniform arrays of quantum dots can be produced, QD lasers may remain temperature sensitive unless the Auger process can also be eliminated.

II. Experiment

A. Samples

The broad area lasers investigated were grown on (100)-Si:GaAs ($n \approx 2 \times 10^{18}$ cm^{-3}) substrates using molecular beam epitaxy. The active regions were embedded between $Al_{0.4}Ga_{0.60}As$ cladding layers (1.6-μm-thick n-type bottom cladding layer and 1.5-μm p-type upper cladding layer) and within an AlGaAs graded index waveguide. A

Manuscript received February 27, 2003; revised August 4, 2003. This work was supported in part by EPSRC.

I. P. Marko is with the Advanced Technology Institute, University of Surrey, Surrey, GU2 7XH, U.K., on leave from the Institute of Physics, National Academy of Sciences of Belarus, 220072 Minsk, Belarus.

A. D. Andreev and A. R. Adams are with the Advanced Technology Institute, University of Surrey, Surrey GU2 7XH, U.K. (e-mail: i.marko@surrey.ac.uk).

R. Krebs, J. P. Reithmaier, and A. Forchel are with the Technische Physik, Universität Würzburg, D-97074, Würzburg, Germany.

Digital Object Identifier 10.1109/JSTQE.2003.819504

short period AlGaAs–GaAs superlattice with varying average Al concentration from 0.30 to 0.15 formed the graded index waveguide layer [12]. The thickness of the waveguide layers was 200 nm in the 1.3-μm QD lasers and 400 nm in the 980-nm QD lasers. The active region of the 980-nm QD lasers was formed by either one or two layers of InAs QDs separated by a 30-nm GaAs spacer [12]. The active region of the 1.3-μm QD lasers consisted of six stacked layers of InAs QDs within 10-nm $Ga_{0.85}In_{0.15}As$ quantum wells (QWs) separated by 40-nm GaAs barriers [13]. The facets were as-cleaved and the cavity lengths were 1 mm for the 980-nm lasers and 2 mm for the 1.3-μm lasers. The width of the top stripe contact for the broad area lasers was 50 or 100 μm. The upper cladding layer in the 4-μm-ridge 1.3-μm QD lasers was etched away up to 250 nm from the inner waveguide [13]. The position of the QD layers inside the QWs was optimized in the ridge lasers. The QD layer in this case was grown on a 1-nm $Ga_{0.85}In_{0.15}As$ layer and covered with a 5-nm layer of the same material. Such optimization appeared to reduce the internal optical losses to 2 cm^{-1} [13]. The substrate in the ridge lasers was thinned to about 150 μm.

B. Investigation of Temperature Behavior of Spontaneous Emission Spectra, Threshold Current $I_{\rm th}$, Radiative Current $I_{\rm rad}$, and Radiative Efficiency

To measure spontaneous emission, a window was milled in the substrate contact of the lasers. The windows were fabricated to a size of approximately 50 $\times$ 200 μm using an Ar-ion-beam milling technique. By this method, we collected pure spontaneous unamplified light. Emissions from the window as well as from the laser facet were collected using 100-μm-diameter core multimoded silica-based optical fibers connected to an optical spectrum analyzer (OSA) or to an optical power meter. To provide a constant collection efficiency of the emission during the measurement cycle, which is essential for the measurements of the temperature dependencies of spontaneous emission, the laser mounts were specifically designed and the optical fibers were carefully clamped and glued to the holder [10], [14]. The temperature was varied from 20 K up to room temperature with an He-refrigerator. The lasers were investigated in pulsed regime to avoid internal heating. The pulse duration and repetition rate were 500 ns and 10–20 kHz, respectively.

During the measurements of the spontaneous emission spectra from the window using an OSA, the total emission from the laser facet was measured using an optical power meter. Thus, the spontaneous emission spectra and output power values at different currents and temperatures were monitored simultaneously. These data were then used for the analysis of temperature behavior of the lasing threshold, the radiative part of the total current $I_{\rm rad}$, and the radiative efficiency η, which characterizes the temperature dependence of a ratio between radiative and nonradiative recombination.

Fig. 1 shows the method for the determination of $I_{\rm rad}$ and η at different temperatures using measured dependencies of the integrated spontaneous emission intensity L versus current. The radiative part of the threshold current is proportional to the radiative recombination rate and thus to the integrated spontaneous emission intensity at the lasing threshold. Therefore, the temperature behavior of $I_{\rm rad}$ was measured using the value of the integrated spontaneous emission intensity L, at threshold. The variation of the radiative recombination efficiency η was determined from the integrated spontaneous emission intensity at a constant subthreshold current. It characterizes the temperature behavior of the radiative recombination rate at a constant rate of carrier injection.

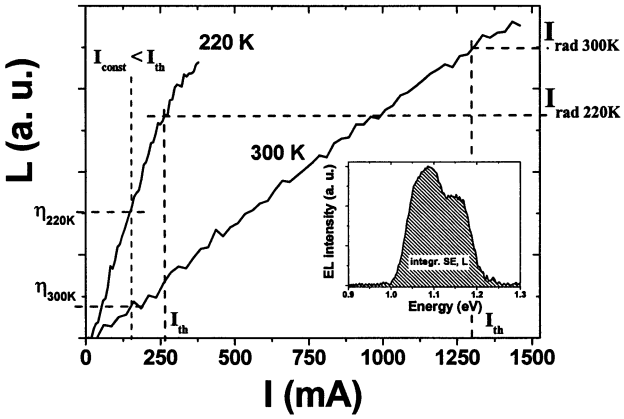

Fig. 1. Method of measurements of the radiative current $I_{\rm rad}$, which is proportional to the integrated spontaneous emission intensity L (see insert), at $I_{\rm th}$ and radiative efficiency η at different temperatures using measured dependencies of the integrated spontaneous emission intensity versus current. Data are shown for the 1.3-μm-broad area QD laser.

To estimate the influence of absorption in the GaAs substrate on the shape of the measured spontaneous emission spectra, the transmission and reflection spectra of a substrate wafer were measured. In addition, spontaneous emission spectra from the window in the top (p-side) contact were measured in the 980-nm QD lasers. The absorption of the thick GaAs substrate wafer was 30%–31% at room temperature in a spectral range 1100–1400 nm. Measurement of the substrate wafer transmittance at the wavelength $\lambda = 1.3$ μm as a function of temperature at $T = 300$–363 K showed that this value is independent of temperature.

Spontaneous emission spectra of the 980-nm QD laser from the window in the top p-side contact and from the bottom side showed that the spectra from the substrate window is modulated by interference. The integrated intensity measured from the substrate side was about 25% less than integrated intensity from the p-side due to absorption of the short wavelength emission. This gives an approximate possible error of the measurements of the temperature behavior of $I_{\rm rad}$ and η, if the absorption changes with temperature. The ratio of the emission spectrum from the top window to the spectrum measured from the bottom side corresponded well to the absorption edge of GaAs. This allowed us to take into account the influence of the absorption in the substrate on the shape of high-energy side of the spontaneous emission spectra from 980-nm lasers.

C. Measurements of $I_{\rm th}$ and Lasing Photon Energy $E_{\rm las}$ Dependencies on Hydrostatic Pressure

High pressure provides a powerful tool to study the recombination mechanisms responsible for laser performance, as was demonstrated for quantum well lasers [10], [11]. Applying high pressure allows the energy $E_{\rm las}$ of the emitted photons to be

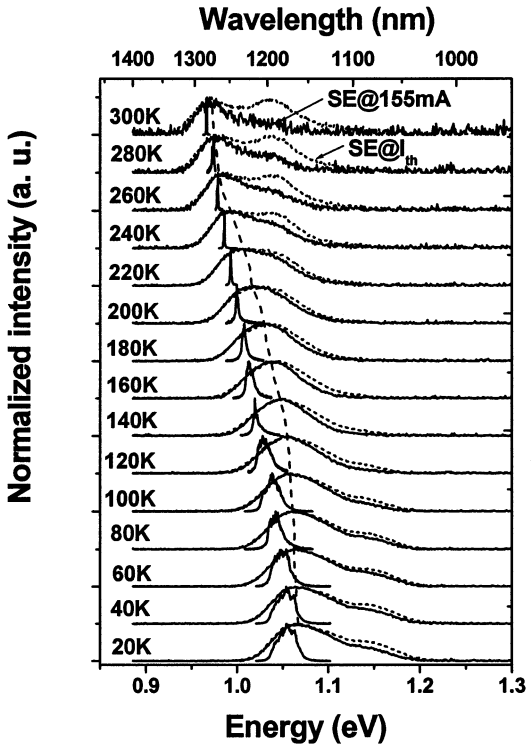

Fig. 2. Spontaneous emission spectra from the window (solid lines correspond to the measurements at injected current $I = 155$ mA which is below the lasing threshold, dotted lines are the spectra at the threshold current) and lasing spectra in a temperature interval of $T = 20$–300 K for the broad area 1.3-μm QD laser. Dashed line shows change of the spontaneous emission peak.

varied while keeping the basic properties of the band structure relatively unchanged. Various recombination mechanisms depend on $E_{\rm las}$ in different ways. For example, the radiative recombination contribution to the laser threshold current usually increases with pressure as $E_{\rm las}^2$ in quantum-well lasers, while the Auger recombination coefficient decreases [10], [11]. In conjunction with other techniques, these variations allow one to determine the relative importance of these recombination mechanisms.

Measurements of the hydrostatic pressure dependence of $I_{\rm th}$ and the lasing photon energy $E_{\rm las}$ were carried out at room temperature using a piston and cylinder apparatus capable of generating 15 kbar [10], [11]. Essence-F was used as the pressure-transmitting medium. The pressure was measured using a coil of manganin wire whose change in resistance with pressure is known. The lasers were aligned with an optical fiber sealed into the upper piston. The lasing wavelength was measured using an optical spectrum analyzer.

III. Experimental Results

A. Temperature Behavior of 1.3-μm and 980-nm QD Lasers

Fig. 2 shows spontaneous emission spectra from the window in the substrate contact and lasing spectra of the broad area 1.3-μm device at different temperatures. To show the temperature variation of spontaneous emission, the spectra measured at a constant current of 155 mA, which is always below lasing threshold, are plotted with solid lines. Spontaneous emission spectra at the threshold current at each temperature are shown with dotted lines. In the whole temperature range from 20 K up to room temperature the lasing spectrum occurred on the low energy side of the spontaneous emission spectrum, which demonstrates that lasing was observed from the ground state. The lasing spectra at low temperature $T < 200$ K were very broad because of inhomogeneous broadening of the gain spectrum due to quantum dot fluctuations. At low temperature lasing threshold conditions were realized for a number of QDs with different emission wavelength. Thus, the full width at half maximum (FWHM) of the lasing spectra was about 25–40 meV at $T = 20$ K. At temperatures higher than 200 K the lasing spectra became much narrower (FWHM of the lasing spectrum at $T = 295$ K was about 2 meV), due to enhanced carrier transfer between QDs and a transition toward an equilibrium carrier distribution between the dots. This process leads to more efficient population of dots of lower energy and to a narrowing of the gain spectrum. This is a reason for the decreasing threshold current with increasing temperature in these lasers, which will be discussed below.

To explain the origin of the high-energy band of the spontaneous emission spectra at low temperature, we considered their variation both with temperature and injected current. We observed several emission peaks in the spontaneous emission spectra of the different 1.3-μm QD lasers. Their positions at $T = 60$ K were about 1.06, 1.09, and 1.17 eV. We attribute the two low-energy emission peaks to transitions via ground state of two ensembles of the dots with different size. It was shown that the energy separation between the ground state emission of developed QDs and small QDs in InAs DWELL structures with 2.0–2.5 ML of InAs can be as big as the difference between the ground and first excited state [15]. Taking into account that all these bands were observable at very low current at low temperature, we think that the recombination via ground state of small QDs and transitions via excited state of developed QDs formed the high-energy band at low temperature. This band, which was observable at low temperature $T < 100$ K, almost vanished in the temperature range from 120 to 220 K (see Fig. 2). With increasing temperature the coupling between QDs improves significantly and carriers recombine in the bigger dots with lower energy states. This leads to the narrowing of the spontaneous emission spectra and to a decrease of the emission bands from the smaller QDs. At the same time, emission from the excited state increases with increasing temperature and becomes very significant at threshold current. Nevertheless, transitions from the smaller QDs also make some contribution to the spontaneous emission spectra, especially under high injected current when lower energy states are filled. This contribution from the smaller dots makes the high-energy band of the spontaneous emission at $T > 220$ K appear more temperature insensitive than the ground state.

The temperature dependence of the spontaneous emission peak energy is shown in Fig. 2 with a dashed line. The red shift of the peak with increasing temperature is faster at $T > 130$ K than the temperature bandgap shrinkage in InAs bulk material. A similar behavior of the luminescence peak has been discussed elsewhere [16], [17]. The temperature enhanced carrier transport in this case allows carriers to move and recombine in the QDs with deeper energy states leading to a decreasing

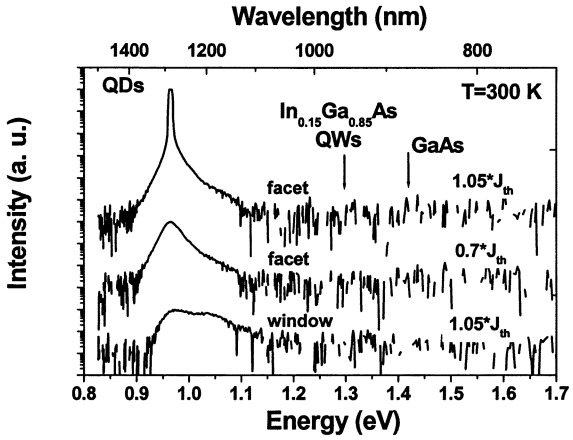

Fig. 3. Emission spectra from the window and from the laser facet at different currents at $T = 300$ K from the 1.3-μm broad area device, demonstrating that there are no emissions from the QWs and barriers.

FWHM of the spontaneous emission spectrum from 80 meV at $T = 20$ K to 64 meV at $T = 180$ K.

Inhomogeneous broadening of the spontaneous emission spectra in the 980-nm QD lasers was not so strong as for the 1.3-μm lasers. The FWHM of the spontaneous emission spectra at $T = 20$ K at low current was 32 and 36 meV for the lasers with one and two QD layers, respectively. The FWHM of the lasing spectra at this temperature was about 10 meV for the laser with one QD layer and about 15 meV for the laser with two QD layers. The lasing spectra became narrower (we observed multimode spectra of about 2 meV width) with increasing temperature as it was observed for the 1.3-μm lasers.

It is also important to note that at room temperature no emission from the QWs and barriers was observable either from the laser facet or from the window in the broad area devices, as shown in Fig. 3. Only a very weak emission was observable in the ridge waveguide laser at 1.27 eV, i.e., the expected region for the $In_{0.15}Ga_{0.85}As$ QW's emission. This indicates that the carriers (electrons and holes) are mainly localized in the dots even at room temperature.

Threshold current densities $J_{\rm th}$, radiative currents $I_{\rm rad}$, and radiative efficiencies η, of both QD lasers with one (solid symbols) and two (crossed symbols) layers of QDs, are given in Fig. 4(a). To compare the temperature behavior of the threshold current and the radiative current, the radiative current was normalized to the threshold current at low temperature ($T < 100$ K) where nonradiative recombination was the smallest. Characteristic temperatures T_0, in the temperature interval $T = 250$–300 K, were as high as $T_0 = 130$ K for the laser with a single QD layer ($\lambda_{300\,\rm K} = 972.4$ nm) and $T_0 = 110$ K for the laser with two QD layers ($\lambda_{300\,\rm K} = 989.5$ nm). At the same time, the radiative part of the total current was relatively independent of temperature even at $T = 150$–300 K, demonstrating that the thermal sensitivity of the lasers is due to a decreasing radiative efficiency.

We observed a very unusual temperature dependence of the threshold current in the broad area 1.3-μm QD lasers with a bump in the temperature interval between 70 and 200 K, which is shown in Fig. 4(b). The radiative current $I_{\rm rad}$, and the radiative efficiency η (both are measured in arbitrary units)

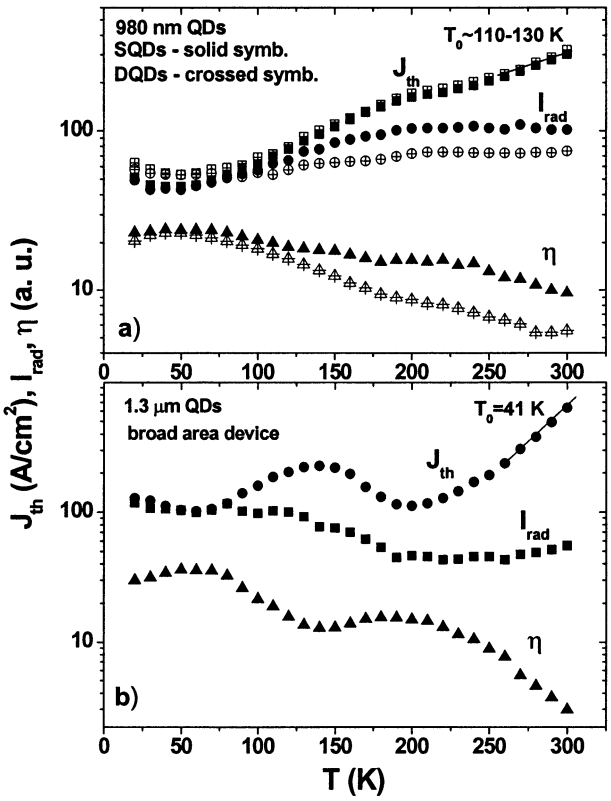

Fig. 4. Temperature dependencies of the threshold current density $J_{\rm th}$, radiative current $I_{\rm rad}$, and radiative efficiency η, for (a) the 980-nm QD lasers with single (SQDs—solid symbols) and double layers of QDs (DQDs—crossed symbols) and (b) for the 1.3-μm broad area QD laser.

are shown as functions of temperature as well. Regions of increasing threshold current, when the radiative current is almost constant, clearly correspond to the decreasing efficiency. This means that the temperature dependence of the lasing threshold is determined by a decrease of the efficiency over these temperature intervals. The decrease of the threshold current and radiative current at temperatures between 150 and 200 K is associated with a decrease in the width of the lasing spectrum and mostly due to a temperature activated process, where carriers are able to transfer and recombine via deeper dot states. A negative characteristic temperature in InAs quantum dots laser diodes has been observed earlier [18]–[20] and also attributed to thermally enhanced carrier transfer between dots.

To understand the recombination mechanisms and loss processes in the QD lasers we have investigated their threshold currents and lasing wavelengths as a function of hydrostatic pressure.

B. Performance of 1.3-μm and 980-nm QD Lasers Studied Using Hydrostatic Pressure

Both 980-nm and 1.3-μm QD structures exhibited similar linear shifts of the lasing photon energy with pressure p. The gradients were $dE_{\rm las}/dp = 10.1$ meV/kbar and $dE_{\rm laser}/dp = 8.3$ meV/kbar for the 980-nm and 1.3-μm QD lasers, respectively [21]. Fig. 5 shows the variation with applied hydrostatic pressure of the threshold current $I_{\rm th}$, for the 980-nm laser with one layer of QDs [Fig. 5(a), solid squares] and for the 1.3-μm lasers [Fig. 5(b), broad area laser—solid squares

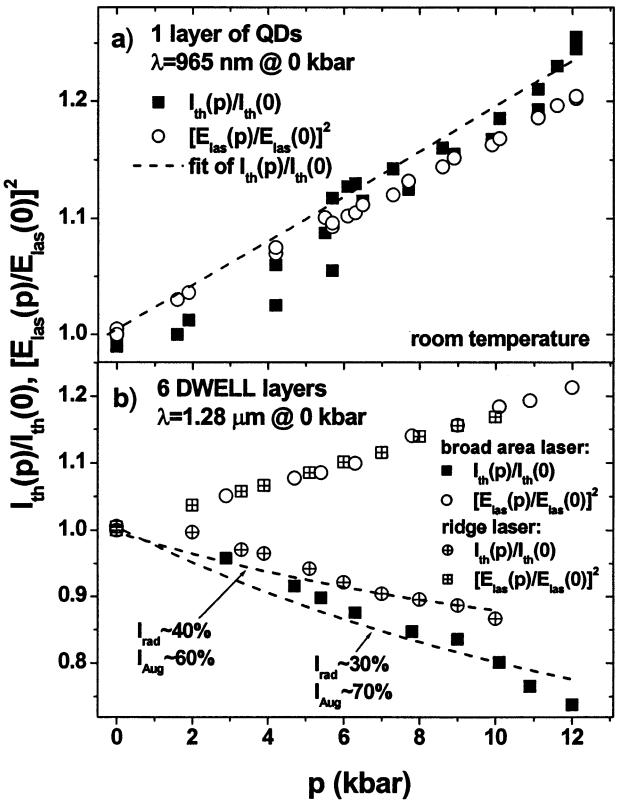

Fig. 5. Normalized threshold current $I_{\rm th}(p)/I_{\rm th}(0)$ and normalized square of the lasing photon energy $[E_{\rm las}(p)/E_{\rm las}(0)]^2$ versus pressure at room temperature (a) for the 980-nm QD laser with one layer of QDs and (b) for the 1.3-μm broad area and ridge waveguide lasers. Dashed lines present fit of the experimental points using (2) to estimate contribution of radiative and Auger recombination processes.

and ridge laser—crossed squares]. The normalized square of the lasing photon energy $[E_{\rm las}(p)/E_{\rm las}(0)]^2$ as a function of pressure is also given in Fig. 5 for each type of laser. For the 980-nm QD lasers, $I_{\rm th}$ increases with pressure proportionally to the square of the photon energy as expected from a simple analytical model of a QD laser with only radiative recombination (see Section IV). However, as shown in Fig. 5(b), the threshold current of the 1.3-μm broad area QD laser decreases by 26% over 12 kbar. This may be compared with the results for 1.3-μm GaInAsP quantum-well lasers where the threshold current decreases by about 10% in the same pressure interval due to a strong Auger recombination contribution of about 50% to the total threshold current [10].

IV. Discussion and Theory

The magnitude of the threshold current density, $J_{\rm th}$ and its variation with temperature in the range around room temperature is of particular practical importance and it is our main concern here. From Fig. 4, where we see that the radiative component of the threshold current $J_{\rm rad}$ is much less temperature sensitive than $J_{\rm th}$, it is clear that there must be at least one temperature-sensitive nonradiative loss process. This is also reflected in the decreasing radiative efficiency η, with increasing temperature, that mirrors the increase in $J_{\rm th}$. Furthermore, from Figs. 4 and 5, it is clear that in the 1.3-μm devices there is a component of the nonradiative loss processes that makes them even more temperature sensitive and that this component decreases strongly with increasing hydrostatic pressure. The mechanisms we have considered are: 1) electron leakage via the AlGaAs cladding layers; 2) intervalence band absorption; 3) thermal excitation from the dots and subsequent nonradiative recombination, probably via defects; and 4) Auger recombination.

Although leakage into the AlGaAs cladding layers, as in 1), can be a major problem in short wavelength devices, it is unlikely to be a problem in these longer wavelength devices where the band-gap difference presents a very large energy barrier. Also, such leakage would be larger in the 980-nm devices than in the 1.3-μm lasers and it is a loss mechanism that increases with increasing pressure [22].

Intervalence band absorption (IVBA) at first appears a likely candidate because it will be stronger in GaAs-based devices than in InP based devices because of the larger spin-orbit splitting. Furthermore, it will be larger in the 1.3-μm lasers than the 980-nm lasers and will also decrease strongly with increasing pressure. However, IVBA affects $J_{\rm th}$ by reabsorbing the laser light as it travels down the laser cavity and it will have a negligible effect on the light observed from the window in the electrode on the n-type substrate. Therefore, although it should not be completely ignored, IVBA cannot explain the large decrease in η which is clearly the main cause for the increase in $J_{\rm th}$.

Thermal excitation from the dots with subsequent nonradiative recombination, as in 3), has been proposed as the major cause of the low T_0 observed on quantum dot lasers and qualitatively it could explain the increase in $J_{\rm th}$ and the decrease in η observed with increasing temperature. The question then arises whether it can also explain the decrease in $J_{\rm th}$ observed with increasing pressure in the 1.3-μm lasers?

To analyze the observed experimental results we have developed a theoretical model based on electronic structure calculations of InAs QDs of pyramidal shape. For calculations of the electron and hole energy spectra and wave functions we used a plane wave expansion method [23], [24]. The three-dimensional (3-D) distributions of the elastic strain and piezoelectric fields in the structure with pyramidal QDs are taken into account using the Green's function method and Fourier transform technique [24], [25]. We assumed that the QD shape is a truncated squared pyramid. The calculations are based on an 8×8 k·p Hamiltonian which incorporates 3-D strain, band mixing, and band anisotropy. The structure parameters and Hamiltonian used are the same as in [26]. Our theoretical analysis includes several steps: 1) calculations of the QD electronic structures and optical matrix elements at various pressures; 2) calculation of laser gain and radiative recombination and analysis of their pressure dependencies; and 3) estimation of the Auger recombination variation with pressure.

As a first step, we calculated the variation of the QD electronic structure with applied hydrostatic pressure. This includes calculations of the electron and hole energy levels and optical transition matrix elements. Fig. 6 shows the calculated dependence on pressure of: 1) the electron and hole energy levels for the ground state in the InAs QDs and for the two-dimensional (2-D) states in the 2-D system consisting of the InGaAs quantum-well and the InAs wetting layer and 2) the optical matrix element for the electron-hole transition between QD ground states. Several important conclusions follow from Fig. 6. Firstly, the energy separation between the ground state in the QD and

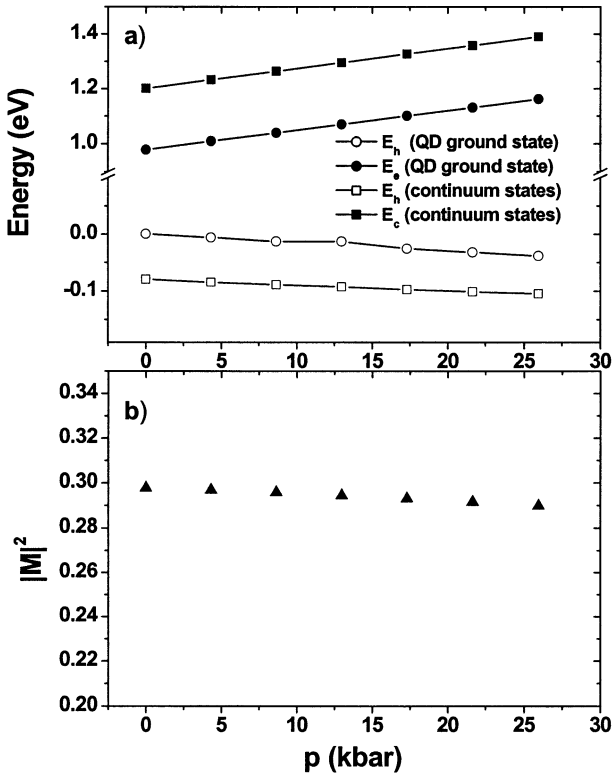

Fig. 6. Calculated varition with pressure of (a) QD ground state energy states and edges of the contiuum states for electrons and holes and (b) squared module of the optical matrix element summed over degenerate spin states, in units of P_0^2 (where P_0 is the interband momentum matrix element, $P_0 = (\hbar/m_0)\langle s|p_x|x\rangle$).

the edge of continuum states in the 2-D system (i.e., the effective barrier heights) for electrons and holes are nearly independent of pressure. From Fig. 6, we also found that the lasing photon energy increases with pressure linearly with $dE_{\rm las}/dp = 8.5$ meV/kbar, which is in very good agreement with our experimental value of 8.3 meV/kbar. Secondly, we found that the square of the optical matrix elements for the ground and several excited transitions do not change significantly (the relative change is less than 1%). This is not surprising since hydrostatic pressure mainly changes only the bandgap, while the band offsets and strain induced spatial variation of the band edges in the structure remains nearly the same. Indeed, this is the reason why hydrostatic pressure is a very convenient and powerful tool to study the nature of carrier recombination in laser structures. Therefore, it can be concluded also that the effect of pressure on the laser performance is mainly due to the variation of the bandgap, i.e., photon lasing energy. Certainly, from Fig. 6 we would not expect sufficient increase with pressure in the binding energy of carriers in the 1.3-μm quantum dots to explain the observed strong decrease in $J_{\rm th}$. However, thermal excitation from the dots and subsequent nonradiative recombination may well explain why $J_{\rm th}$ is more temperature sensitive than $J_{\rm rad}$ in the 980-nm dots and it is interesting to estimate the magnitude of this effect. If we assume that only radiative recombination and thermal excitation are responsible for the threshold current in the 980-nm dots and also that thermal excitation from the dots will be negligible at temperatures below 100 K, then we can normalize $I_{\rm rad}$ to $J_{\rm th}$ in this temperature range (see Fig. 4) and so determine an absolute value for $I_{\rm rad}$ up to room temperature. This shows that at 300 K, the contributions to $J_{\rm th}$ for the radiative and thermal-escape currents are 60% and 40%, respectively (we took into account here the error of $I_{\rm rad}$ due to absorption of spontaneous emission in the substrate). The fact that $J_{\rm th}$ increases with pressure in the 980-nm devices even with 40% thermal leakage supports our theoretical model for the pressure variation of the levels in the 1.3 μm dots where the confining structures are not very different. It is also important to note that η decreases much more quickly with increasing temperature in the 1.3-μm lasers than in the 980-nm devices, which is contrary to what one would expect if the confining energy were small and thermal loss large in the 1.3-μm lasers. These arguments lead us finally to the conclusion that it is Auger recombination that is likely to be the mechanism that is responsible for the much lower T_0 in 1.3-μm than 980-nm devices and we now consider its magnitude.

Auger recombination 4) is a very complex process and detailed discussion must be left to a further publication. However, previous work has shown that it is an important mechanism in 1.3-μm quantum well lasers and explains the dependence of their $J_{\rm th}$ on temperature and pressure.

Below, we show that in QDs the radiative current and the Auger current depend in opposite ways on the photon lasing energy $E_{\rm las}$: the radiative current *increases* with $E_{\rm las}$, while the Auger current decreases with $E_{\rm las}$. Therefore, by analyzing the dependence of the laser threshold current on hydrostatic pressure, we can estimate the fractions of the radiative and Auger currents in the total threshold current. The same approach was shown to be very powerful for QW lasers [27].

The second step of our calculations was to calculate the gain and the threshold carrier density as a function of pressure. The gain was calculated using the following expression:

$$g(\omega) = \frac{4\pi^2}{n}\frac{e^2\Gamma_{\rm opt}}{\hbar^2\omega c}\frac{N_{\rm QD}}{d} \times \sum_{n_e,n_h}\langle|M_{\rm eh}|^2(f_e+f_h-1)L(E_{\rm eh}-\hbar\omega)\rangle \quad (1)$$

where n is the refractive index of the QD material, e is the electron charge, c is the velocity of light in vacuum, ω is the light frequency, $N_{\rm QD}$ is the 2-D in-plane density of QDs, d is the total width of the active region, $M_{\rm eh}$ is the optical matrix element for the transition with energy $E_{\rm eh}$ between the electron level $n_{\rm e}$ and hole level n_h, over which the summation is taken, f_e and $f_{\rm h}$ are the distribution functions, L is the line-shape function, and the brackets in (1) mean the averaging over the size distribution over QDs.

Let us now analyze the pressure dependence of the gain. Since the optical matrix element $M_{\rm eh}$ is nearly constant with pressure, then at a fixed carrier density N, the peak gain g depends on pressure through the change in $E_{\rm las}$. From (1), it then follows that the peak gain is inversely proportional to the energy $E_{\rm las}$, $g \propto 1/E_{\rm las}$, i.e., the gain decreases with pressure at fixed carrier density N. It should be noted that we consider here only the case of room temperature and assume that the carriers in QDs are in equilibrium and, therefore, can be described by a Fermi–Dirac distribution.

To calculate the threshold carrier density $N_{\rm th}$ at a given pressure (i.e., given $E_{\rm las}$) we must solve the threshold condition,

$g(N_{\rm th}, E_{\rm las}) = \alpha_i(N_{\rm th}, E_{\rm las}) + \alpha_M$, where α_i are the total internal losses and α_M are the mirror losses. In the general case, the calculated dependence of $N_{\rm th}$ on pressure is quite sensitive to the variation of the internal losses with $E_{\rm las}$, because the internal losses usually decrease with increasing $E_{\rm las}$ (since they are mainly caused by the intervalence band absorption in various areas). In our analysis here, it is, however, not so important since the total internal losses appear to be quite low at room temperature [13]. Therefore, even if the internal losses vanish at high pressure, we still find $N_{\rm th}$ increases as function of pressure (or $E_{\rm las}$), because the peak gain is decreasing as $g \propto 1/E_{\rm las}$. In summary, we found that the threshold carrier density $N_{\rm th}$ increases with pressure.

The next step is the calculation of the radiative current $I_{\rm rad}$ dependence on pressure. The calculated radiative current density at zero pressure and 300 K for the 1.3-μm devices is 150 A/cm^2, which accounts for only 24% of the total threshold current measured. This indicates that an additional recombination channel indeed exists in these devices.

Let us now analyze the pressure dependence of the radiative current at threshold, $I_{\rm rad}$. This dependence is determined by two factors: 1) pressure dependence of the radiative recombination coefficient B (i.e., the radiative recombination rate at fixed carrier density) and 2) pressure dependence of the threshold carrier density $N_{\rm th}$. We note that in quantum wells it is commonly assumed that $I_{\rm rad} = BN_{\rm th}^2$; however, in QDs we have $I_{\rm rad} = B(N_{\rm th})^\beta$, where $1 < \beta < 2$ [28]. The radiative recombination coefficient B is proportional to the lasing energy (see [29, (5b)]), $B \propto E_{\rm las}$, because the optical matrix is nearly independent of pressure as discussed above. As we discussed above, $N_{\rm th}$ increases with pressure. Since $I_{\rm rad} = B(N_{\rm th})^\beta$, we, therefore, conclude that the radiative current $I_{\rm rad}$ increases with pressure even faster than $E_{\rm las}$ because the threshold carrier density increases with pressure as well. The calculated variation of $I_{\rm rad}(p)$ depends on the QD shape, composition distribution, and other structure parameters, which are either unknown (for example we do not know the spatial variation of the In composition around the QD) or are known with quite big uncertainty (for example it is difficult to measure or calculate the dependence of the internal losses with pressure). Nevertheless, we can definitely say that in the studied QD structure $I_{\rm rad}$ increases with $E_{\rm las}$ (or pressure) as $I_{\rm rad} \propto E_{\rm las}^l$, where $l > 1$ (because $N_{\rm th}$ increases with pressure). This conclusion is supported by the observed variation for the 980-nm devices, where $l = 2$ was observed.

We will now consider why the rates of Auger processes decrease quickly with $E_{\rm las}$ with increasing pressure. A detailed calculation of the Auger rate in QDs is a subject of our future research, only qualitative analysis is presented here.

The Auger recombination coefficient C (i.e., the Auger rate at fixed carrier density) is determined by the square module of the Coulomb matrix element $M_{\rm Col}, C \propto |M_{\rm col}|^2$. In its turn, $M_{\rm col}$ is proportional to the product of two overlap integrals $I_{\rm eh}$ and $I_{\rm ex}, |M_{\rm col}| \propto |I_{\rm eh}||I_{\rm ex}|$. The first overlap integral $I_{\rm eh}$ is between the electron and hole states localized in the QDs. The second overlap integral $I_{\rm ex}$ is between the carrier (electron or hole—depending on the type of the Auger process) localized in the QD and a highly excited carrier in the continuum spectrum. The electron states in the QD are mostly s-type (conduction band related Bloch functions), while the hole states are mainly p-type (valence band related Bloch functions). Therefore, the overlap integral $I_{\rm eh}$ is determined by the admixture of the p-type Bloch components to the electron states in the QD or by the admixture of the s-type Bloch components to the hole states in the QD (the latter was found to be several times less effective). The degree of this admixture decreases with pressure and it is approximately proportional to $(E_o/E_{\rm las})^{1/2}$, where E_o is the electron level in QD measured from the unstrained conduction band edge of InAs. So, we can conclude that $I_{\rm eh}$ decreases with $E_{\rm las}$ as $I_{\rm eh} \propto E_{\rm las}^{-1/2}$. In fact, numerical calculations show that $I_{\rm eh}$ decreases even faster. The overlap integral $I_{\rm ex}$ is between the state in the QD and highly excited state in the continuum. The wavefunction of the state localized in the QD varies relatively "smoothly" (with the characteristic size of such variation of order of the QD dimension), but the wave function of highly excited states is a quickly oscillating function of the spatial coordinates. Therefore, the overlap between these two states is also small and it decreases with $E_{\rm las}$ as $I_{\rm ex} \propto E_{\rm las}^{-1/2}$ or faster. Thus, we find that the square of the Coulomb matrix element decreases with $E_{\rm las}$ as $E_{\rm las}^{-2}$ or faster. According to our numerical analysis the Auger coefficient C decreases with $E_{\rm las}$ as $C \propto E_{\rm las}^{-m}$, where m is between 3 and 8; the value of m depends on the QD shape, size, and composition.

The final step of our calculations is a rough estimation of the Auger current contribution to the total threshold current. For this purpose, we assume that the laser threshold current consists of only radiative and Auger recombination terms, $I_{\rm th} = I_{\rm rad} + I_{\rm Aug}$, where $I_{\rm rad}$ is proporational to $E_{\rm las}^l$, the Auger contribution $I_{\rm Aug}$ varies as $I_{\rm Aug} \propto (E_{\rm laser})^{-m}$. We finally assume that $x = I_{\rm rad}(0)/I_{\rm th}(0)$ is the fraction that radiative recombination contributes to $I_{\rm th}$ at zero pressure. For the threshold current variation with pressure we then find that [21]

$$I_{\rm th}(p)/I_{\rm th}(0) = x\varepsilon^l + (1-x)\varepsilon^{-m} \qquad (2)$$

where $\varepsilon = E_{\rm las}(P)/E_{\rm las}(0)$ is the relative variation of the lasing photon energy with pressure, which is measured to be around 1.1 at 12 kbar. We then use (2) to fit the experimentally measured variation of $\rm I_{th}$ with pressure, and the result is shown in Fig. 5. We found the fraction of the radiative current is 30% and 40% for the broad area and ridge 1.3-μm devices, respectively [see Fig. 5(b)]. This simple model ignores thermal escape current and gives the fraction of the radiative current of 100% for the 980-nm device [see Fig. 5(a)]. These values were obtained assuming that $l = 2$ and $m = 11/2$ as in QW lasers [30]. It is interesting to note that these estimations agree very well with the value of the directly calculated radiative current of 24% of $I_{\rm th}$ for the 1.3-μm broad area laser. If, as discussed above, we use other values of l between 1 and 3 and m between 3 and 8, then we always get that the fraction of the Auger contribution to the total threshold current is greater than 58%. Thus, from analysis of the high-pressure measurements we believe that the Auger process dominates over radiative recombination at room temperature in the 1.3 μm devices studied. In contrast, in the 980-nm lasers radiative recombination dominates and the Auger current is negligible.

V. Conclusion

In conclusion, we have shown that while the radiative current in both our 1.3-μm and 980-nm wavelength quantum dot lasers

is indeed relatively temperature insensitive, the total threshold current includes significant temperature dependent nonradiative recombination. Furthermore, in order to explain both the temperature and pressure dependences of the longer wavelength devices it is necessary to include Auger recombination just as in bulk and quantum well devices operating at 1.3 μm. This implies that, even if perfectly uniform arrays of quantum dots can be produced, QD lasers will remain temperature sensitive unless the Auger processes can be eliminated.

ACKNOWLEDGMENT

The authors gratefully acknowledge Dr. S. Sweeney for helpful discussions and EPSRC for financial support.

REFERENCES

[1] Y. Arakawa and H. Sakaki, "Multidimensional quantum well laser and temperature dependence of its threshold current," *Appl. Phys. Lett.*, vol. 40, no. 11, pp. 939–941, 1982.

[2] M. Asada, Y. Miyamoto, and Y. Suematsu, "Gain and threshold of three dimensional quantum box laser," *IEEE J. Quantum Electron.*, vol. 22, pp. 1915–1921, Sept. 1986.

[3] K. Mukai, Y. Nakata, K. Otsubo, M. Sugawara, N. Yokoyama, and H. Ishikawa, "1.3 μm CW lasing characteristics of self-assembled InGaAs-GaAs quantum dots," *IEEE J. Quantum Electron.*, vol. 36, pp. 472–478, Apr. 2000.

[4] V. M. Ustinov and A. E. Zhukov, "Topical review: GaAs-based long-wavelength lasers," *Semicond. Sci. Technol.*, vol. 15, pp. R41–R54, 2000.

[5] A. R. Kovsh, A. E. Zhukov, N. A. Maleev, S. S. Mikhrin, V. M. Ustinov, A. F. Tsatsul'nikov, M. V. Maksimov, B. V. Volovik, D. A. Bedarev, Yu. M. Shernyakov, E. Yu. Kondrat'eva, N. N. Ledentsov, P. S. Kop'ev, Zh. I. Alferov, and D. Bimberg, "Lasing at a wavelength close to 1.3 μm in InAs quantum-dot structures," *Semicond.*, vol. 33, no. 8, pp. 929–932, 1999.

[6] L. V. Asryan and R. A. Suris, "Temperature dependence of the threshold current density of a quantum dot laser," *IEEE J. Quantum Electron.*, vol. 34, pp. 841–850, May 1998.

[7] M. Grundmann, O. Stier, S. Bognar, C. Ribbat, F. Heinrichsdorff, and D. Bimberg, "Optical properties of self-organized quantum dots: Modeling and experiments," *Phys. Stat. Sol. (a)*, vol. 178, pp. 255–262, 2000.

[8] O. B. Shchekin, G. Park, D. L. Huffaker, and D. G. Deppe, "Discrete energy level separation and the threshold temperature dependence of quantum dot lasers," *Appl. Phys. Lett.*, vol. 77, pp. 466–468, 2000.

[9] O. B. Shchekin and D. G. Deppe, "Low-threshold high-T_0 1.3-μm InAs quantum dot lasers due to p-type modulation doping of the active region," *IEEE Photon. Technol. Lett.*, vol. 14, pp. 1231–1233, Sept. 2002.

[10] T. Higashi, S. J. Sweeney, A. F. Phillips, A. R. Adams, E. P. O'Reilly, T. Uchida, and T. Fujii, "Experimental analysis of temperature dependence in 1.3-m AlGaInAs-InP strained MQW lasers," *IEEE J. Select. Topics Quantum Electron.*, vol. 5, pp. 413–419, Mar. 1999.

[11] S. J. Sweeney, T. Higashi, A. Andreev, A. R. Adams, T. Uchida, and T. Fujii, "Superior temperature performance of 1.3 μm AlGaInAs-based semiconductor lasers investigated at high pressure and low temperature," *Phys. Stat. Sol. (b)*, vol. 223, no. 2, pp. 573–578, 2001.

[12] F. Schäfer, B. Mayer, J. P. Reithmaier, and A. Forchel, "High-temperature properties of GaInAs/AlGaAs lasers with improved carrier confinement by short-period superlattice quantum well barriers," *Appl. Phys. Lett.*, vol. 73, no. 20, pp. 2863–2865, 1998.

[13] R. Krebs, F. Klopf, J. P. Reithmaier, and A. Forchel, "High performance 1.3 μm quantum-dot lasers," *Jpn. J. Appl. Phys.*, vol. 41, pp. 1158–1161, 2002.

[14] A. F. Phillips, S. J. Sweeney, A. R. Adams, and P. J. A. Thijs, "The temperature dependence 1.3- and 1.5 μm compressively strained InGaAs(P) MQW semiconductor lasers," *IEEE J. Select. Topics Quantum Electron.*, vol. 5, pp. 401–412, Mar. 1999.

[15] M. V. Maximov, A. F. Tsatsul'nikov, B. V. Volovik, D. A. Bedarev, Yu. M. Shernyakov, I. N. Kaiander, E. Yu. Kondrat'eva, A. E. Zhukov, A. R. Kovsh, N. A. Maleev, S. S. Mikhrin, V. M. Ustinov, Yu. G. Musikhin, P. S. Kop'ev, Zh. I. Alferov, R. Heitz, N. N. Ledentsov, and D. Bimberg, "Optical properties of quantum dots formed by activated spinodal decomposition for GaAs-based lasers emitting at ~ 1.3 μm," *Microelectronic Eng.*, vol. 51–52, pp. 61–72, 2000.

[16] L. Brusaferri, S. Sanguinetti, E. Grilli, M. Guzzi, A. Bignazzi, F. Bogani, L. Carraresi, M. Colocci, A. Bosacchi, P. Frigeri, and S. Franchi, "Thermally activated carrier transfer and luminescence line shape in self-organized InAs quantum dots," *Appl. Phys. Lett.*, vol. 69, no. 22, pp. 3354–3356, 1996.

[17] S. Sanguinetti, M. Henini, M. G. Alessi, M. Capizzi, P. Frigeri, and S. Franchi, "Carrier thermal escape and retrapping in self-assembled quantum dots," *Phys. Rev. B*, vol. 60, no. 11, pp. 8276–8283, 1999.

[18] A. E. Zhukov, V. M. Ustinov, A. Yu. Egorov, A. R. Kovsh, A. F. Tsatsulnikov, N. N. Ledentsov, S. V. Zaitsev, N. Yu. Gordeev, P. S. Kop'ev, and Zh. I. Alferov, "Negative characteristic temperature of InGaAs quantum dot injection laser," *Jpn. J. Appl. Phys.*, pt. 1, vol. 36, no. 6B, pp. 4216–4218, 1997.

[19] A. Patane, A. Polimeni, M. Henini, L. Eaves, P. C. Main, and G. Hill, "$In_{0.5}Ga_{0.5}As$ quantum dot lasers grown on (100) and (311)B GaAs substrates," *Cryst. Growth*, vol. 201–202, pp. 1139–1142, 1999.

[20] M. Grundmann, O. Stier, S. Bognar, C. Ribbat, F. Heinrichsdorff, and D. Bimberg, "Optical properties of self-organized quantum dots: Modeling and experiments," *Phys. Stat. Sol. (a)*, vol. 178, pp. 255–262, 2000.

[21] I. P. Marko, A. D. Andreev, A. R. Adams, R. Krebs, J. P. Reithmaier, and A. Forchel, "High-pressure studies of the recombination processes, threshold currents and lasing wavelength in InAs/GaInAs quantum dot lasers," *Phys. Stat. Sol. (b)*, vol. 235, no. 2, pp. 407–411, 2003.

[22] P. Blood, E. D. Fletcher, K. Woodbridge, K. C. Heasman, and A. R. Adams, "Influence of the barriers on the temperature dependence of the threshold current in GaAs/AlGaAs quantum well lasers," *IEEE J. Quantum Electron.*, vol. 25, p. 1459, 1989.

[23] A. D. Andreev, "Modeling of gain for lasers based on CdSe planar QD-system in ZnMgSSe matrix," in *In-Plane Semiconductor Lasers: From Ultraviolet to Mid-Infrared, Proc. SPIE*, H. K. Choi and P. S. Zory, Eds., 1998, vol. 3284, pp. 151–161.

[24] A. D. Andreev and E. P. O'Reilly, "Theory of the electronic structure of GaN/AlN hexagonal quantum dots," *Phys. Rev. B*, vol. 62, pp. 15 851–15 870, 2000.

[25] A. D. Andreev, J. R. Downes, D. A. Faux, and E. P. O'Reilly, "Strain distributions in quantum dots of arbitrary shape," *J. Appl. Phys.*, vol. 84, no. 1, pp. 297–305, 1999.

[26] O. Stier, M. Grundmann, and D. Bimberg, "Electronic and optical properties of strained quantum dots modeled by 8-band kp theory," *Phys. Rev. B*, vol. 59, pp. 5688–5701, 1999.

[27] S. J. Sweeney, T. Higashi, A. R. Adams, T. Uchida, and T. Fujii, "Improved temperature dependence of 1.3 μm AlGaInAs-based MQW semiconductor diode lasers revealed by hydrostatic pressure," *Electron. Lett.*, vol. 34, no. 22, pp. 1231–1233, 1998.

[28] A. Andreev, "Radiative recombination dependence on carrier density in QDs," in *A One Day Meeting "Growth, Characterization, and Physics of Semiconductor Quantum Dots"*. Sheffield, U.K.: Univ. Sheffield, Jan. 22, 2003.

[29] L. V. Asryan and R. A. Suris, "Inhomogeneous line broadening and the threshold current density of a semiconductor quantum dot laser," *Semicond. Sci. Technol.*, vol. 11, pp. 554–567, 1996.

[30] G. G. Zegrya, A. D. Andreev, N. A. Gun'ko, and E. V. Frolushkina, "Calculation of QW-laser threshold currents in terms of new channels of nonradiative Auger recombination," in *Physics and Simulation of Optoelectronic Devices III, Proc. SPIE*, M. Osinski and W. W. Chow, Eds., 1995, vol. 2399, pp. 307–316.

I. P. Marko, photograph and biography not available at time of publication.

A. D. Andreev, photograph and biography not available at time of publication.

A. R. Adams, photograph and biography not available at time of publication.

R. Krebs, photograph and biography not available at time of publication.

J. P. Reithmaier, photograph and biography not available at time of publication.

A. Forchel, photograph and biography not available at time of publication.